

CO₂ Selective Water Gas Shift Membrane Reactor : Modeling and Simulation

Sang Kompiang Wirawan^{*,1}

*Derek Creaser*²

*I Made Bendiyasa*¹

*Wahyudi Budi Sediawan*¹

¹Department of Chemical Engineering, Faculty of Engineering, Gadjah Mada University, 55281, Yogyakarta, Indonesia

²Chemical Reaction Engineering, Chalmers University of Technology, SE-412 96, Gothenburg, Sweden

*e-mail: skwirawan@chemeng.ugm.ac.id

The concept of a CO₂ selective water gas shift (WGS) membrane reactor has been modeled and simulated by a one-dimensional reactor and transport process in the membrane. The model was used to investigate the effect of temperature, total pressure, membrane thickness and area on the reactor performance. A Silicalite-1 membrane was considered to be integrated with the WGS reactor. The mass transport through the membrane was described by surface diffusion. Air was used as sweep gas on the permeate side of the membrane. The catalytic WGS kinetics were for a commercial Cu/ZnO catalyst for the lower-temperature WGS reaction. The WGS membrane reactor was sized to produce H₂ sufficient for the production of 10 kW electrical power from a fuel cell. The modeling and simulation results showed that the WGS membrane reactor with a silicalite-1 membrane was capable of decreasing the CO concentration to about 675 ppm which is 70% less than that achievable at equilibrium conversion, but it would come at the cost of unacceptable H₂ loss. Based on a minimum target of H₂ loss, the optimum outlet CO concentration achieved by the silicalite-1 membrane reactor was about 1310 ppm, under a range of limited conditions. The modeling study showed that both the WGS reaction rate and the CO₂/H₂ selective permeation played an important role on the overall reactor performance.

Keyword: CO₂ selective membrane, Water Gas Shift, General Maxwell-Stefan, Modeling

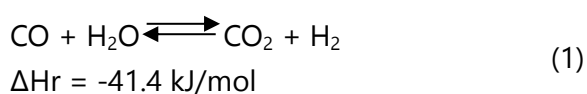
INTRODUCTION

A fuel processor for hydrogen production for a Polymer Electrolyte Membrane (PEM) fuel cell might consist of the following parts; a reforming reactor, one or more water-gas shift (WGS) reactors and finally a preferential CO oxidation (PrOx) reactor. The WGS and

PrOx reactors comprise a clean-up process that reduces the CO concentration in the reformat gas, because CO poisons the platinum electrocatalyst of the fuel cell. The CO concentration must be reduced to at least less than 100 ppm for satisfactory performance of the fuel cell. It has been estimated that such a clean-up process

would comprise about 80% of the total reactor volume of the fuel processor (Zalc and Löffler, 2002), making it highly inconvenient especially for portable applications, such as onboard vehicles. The commercial introduction of portable fuel processors for PEM fuel cells may hinge on the development of a more efficient CO clean-up process.

The WGS converts CO in the synthesis gas from the reformer and generates more H₂ as described in the following reaction,



The WGS reaction is reversible and exothermic, so that it is thermodynamically unfavorable at elevated temperatures. Breaking the WGS reaction equilibrium by a H₂ or CO₂ selective membrane reactor could reduce the required size or number of WGS reactors or possibly eliminate the need for a PrOx reactor step.

Some modeling studies of H₂ and CO₂ selective membrane reactors were published recently (Basile *et al*, 2003, Brunetti *et al*, 2007, Huang *et al*, 2005). Although H₂ selective membranes produce high purity H₂, due to low permeance, a large membrane area might be needed to achieve a suitable H₂ flow to feed the fuel cell. A CO₂-selective

WGS membrane reactor has the advantage that a reformat gas with a CO concentration lower than that obtainable from equilibrium of the WGS reaction could be obtained, if air or steam were used as sweep gas on the permeate side of the membrane to obtain a driving force for the separation. In addition the capacity of a H₂ separation membrane would have to be larger than that of a CO₂ separation membrane since the concentration of H₂ in the reformat gas is approximately three times greater than that of CO₂.

A schematic of the membrane reactor considered here is shown in Figure 1. The membrane encloses the catalyst. The WGS takes place on the catalyst and CO₂ permeates selectively through the membrane to the so-called permeate side. Removing CO₂ from the reaction zone forces the chemical equilibrium of the reaction to the product side. The sweep gas on the shell side reduces the CO₂ concentration and increases the trans-membrane partial pressure difference providing a driving force. After reaction, the product stream leaves the reactor as the retentate stream, which is a high H₂ flow rate with a low concentration of CO and more importantly with a CO concentration lower than the equilibrium for the WGS reaction.

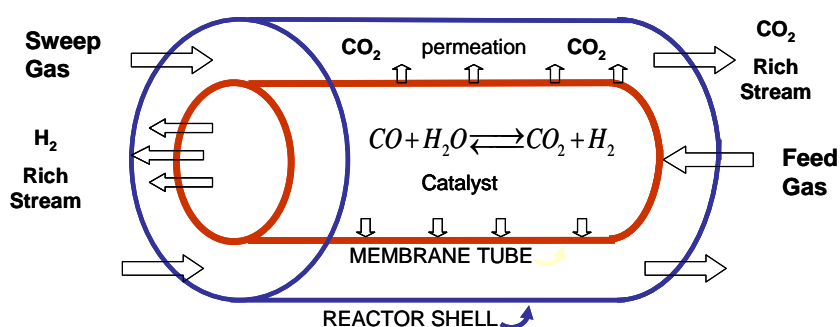


Figure 1. The CO₂ selective WGS membrane reactor concept

Several materials have good potential for developing membrane applications. MFI membranes are currently thought to have good potential because of their relatively high permeability and thermal stability. Among zeolite-based membranes, the developments of techniques to synthesize MFI membranes have advanced the furthest, i.e. methods to reproducibly synthesize membranes of high quality (few defects) and selective permeability. However, the development of most materials is still at the laboratory scale with typical sample sizes of several cm² (Graaf *et al*, 1999, Hedlund *et al*, 2002, Huang *et al*, 2005, Kapteijn *et al*, 1995).

A modeling study of CO₂-selective WGS membrane reactors including the system parameters such as CO₂/H₂ separation, CO₂ permeability, and sweep-to-feed molar flow rate ratio has been carried out by J. Huang, *et al* (2005). Here we extend this study by including the performance of an actual membrane material, namely an MFI zeolite based membrane, into an examination of the feasibility of a CO₂-selective membrane reactor.

In the present work, a silicalite-1 membrane is integrated into a WGS membrane reactor model to demonstrate how the mass transport parameters such as adsorption and diffusion have a significant influence on transport selectivity in the membranes and eventually on the performance of a CO₂ selective membrane WGS reactor. A silicalite-1 membrane was selected for the following reasons:

1. Among zeolite membranes methods to produce them have advanced significantly and in addition the membrane transport parameters have

been rather extensively studied experimentally and by simulation models (Algieri *et al*, 2003, Ciavarella *et al*, 2000, Krishna and Baur, 2003, Krishna and Wesselingh, 1997, Miachon *et al*, 2007).

2. It has been demonstrated that they are selective for separation of CO₂ from CO₂/H₂ mixtures under low temperature when surface diffusion dominates transport and the adsorption of CO₂ is favored over that of H₂ (Kapteijn *et al*, 1995).
3. The required adsorption and diffusion parameters for the relevant components in silicalite-1 are widely reported in the literature

The General Maxwell-Stefan (GMS) theory for surface diffusion was used to describe the multi-component mass transport across the membranes in the WGS-membrane reactor. The adsorption and diffusion parameters were provided by our earlier experimental results and combined with some parameters taken from literature.

MODEL DESCRIPTION

The CO₂ selective WGS membrane reactor is modeled by a one-dimensional reactor and transport process in the membrane. The following assumptions are made in the model:

1. the reactor operates isothermally and at a steady state
2. axial mixing is negligible
3. the axial total pressure drops on both permeate and retentate sides are negligible
4. transport through defects in the

- silicalite-1 membrane is negligible
5. transport resistance due to a membrane support material is neglected
 6. only surface diffusion is included in the membrane transport, other transport mechanisms such as gas translational diffusion are neglected

The WGS membrane reactor is sized for the production of H₂ corresponding to the generation of 10 kW electrical power from the fuel cell with typical feed concentrations that could be obtained from the auto-thermal steam reforming of diesel fuel. The feed composition entering the reactor is listed in Table 1. The total molar flowrate, n_{tot} was 0.13 mol/s. The catalyst was assumed to be a commercial Cu/ZnO catalyst for the lower-temperature WGS reaction. A reaction rate expression from Keiski *et al* (1993) was chosen.

The reaction rate, r_i is given by the following equation:

$$r_i = 1.0 \times 10^{-3} \frac{\rho_b P}{n_{tot} RT} \exp\left(13.39 - \frac{5557}{T}\right) n_{CO} \left(1 - \frac{n_{H_2} n_{CO_2}}{K_T n_{CO} n_{H_2O}}\right) \quad (2)$$

Where n is molar flowrate, P is total pressure, ρ_b is catalyst bulk density and K_T the expression for the equilibrium constant (Salmi and Hakkarainen, 1989) for the WGS reaction, which is a function of temperature T ,

$$K_T = \exp\left(\frac{4577.8}{T} - 4.33\right) \quad (3)$$

The schematic drawing of the mass balance

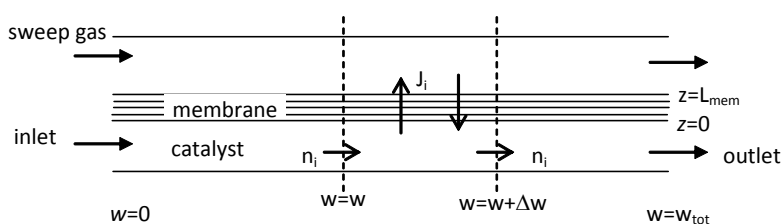


Figure 2. Schematic drawing of mass balance in the membrane reactor

in the membrane reactor is depicted in Figure 2.

Based on the reactor mass balance and considering an isothermal process, the molar flow rate of each component can be expressed as:

$$\frac{dn_i}{dw} = r_i - A_s J_i \quad (4)$$

Where w is weight of the catalyst, A_s is the area of the membrane per catalyst mass and J_i is molar flux.

Tabel 1. Typical gas composition of autothermal steam reforming syngas

| Gases | Composition (%) |
|------------------|-----------------|
| CO | 9.9 |
| H ₂ O | 22.0 |
| H ₂ | 36.3 |
| CO ₂ | 9.5 |
| CH ₄ | 0.2 |
| N ₂ | 22.1 |

In this study, a relatively thick silicalite-1 membrane is considered (10-60 μm), thus the transport resistance through the support can be assumed to be negligible compared to that in the zeolite membrane (Wirawan *et al*, 2011). The mass transport mechanism applied for the membrane is surface diffusion. Under the conditions for the low temperature WGS reaction (150 – 250°C),

Tabel 2. Adsorption and Diffusion parameters

| Parameters | H ₂ | CO ₂ | CO | H ₂ O | N ₂ | O ₂ | CH ₄ |
|---|-----------------------------|-----------------------------|-----------------------------|----------------------------|----------------------------------|----------------------------|----------------------------|
| Adsorption | Bakker <i>et al</i> (1997) | Wirawan and Creaser (2006a) | Wirawan <i>et al</i> (2009) | Fleys and Thompson (2005) | Dunne <i>et al</i> (1996) | Dunne <i>et al</i> (1996) | Dunne <i>et al</i> (1996) |
| q_{sat} [mol/kg] | 5.4 | 2.025 | 0.83 | 14.525 | 1.152 | 1.251 | 2.208 |
| $-\Delta H_0$ [kJ/mol] | 5.9 | 23.6 | 13.6 | 32.38 | 18.56 | 14.13 | 20.75 |
| $-\Delta S_0$ [J/mol/K] | 43 | 74.9 | 52.8 | 127.09 | 75.4 | 62.94 | 77.28 |
| Surface Diffusion | Wirawan <i>et al</i> (2011) | Wirawan <i>et al</i> (2011) | Kärger <i>et al</i> (1993) | Bussai <i>et al</i> (2002) | Papadopoulos <i>et al</i> (2004) | Nagumo <i>et al</i> (2001) | Skoulidas and Sholl (2002) |
| D_0^S [$\times 10^{-8}$ m ² /s] | 2.1 | 1.70 | 8.00 | 6.20 | 3.10 | 4.01 | 8.06 |
| $-E_0^S$ [kJ/mol] | 4.78 | 10.6 | 5.00 | 7.26 | 2.67 | 3.00 | 4.25 |

gas translational diffusion is negligible compared to the surface diffusion. Generally gas translational diffusion becomes significant only at higher temperature. (Ciavarella *et al*, 2000, Miachon *et al*, 2007, Wirawan *et al*, 2011). The adsorption and diffusion parameters used in the membrane transport model are listed in Table 2.

The General Maxwell-Stefan diffusion formulation was applied for describing the multi-component surface diffusion, where the following equations were adapted from Krishna and Baur (2003) and Krishna and Wesselingh (1997). The surface diffusion flux J^S was expressed in the ($nc \times nc$) dimensional matrix form,

$$(J^S) = -\rho[q_{sat}] [B]^{-1} [\Gamma] \nabla(\theta) \quad (5)$$

The occupancy θ_i is defined by the adsorption equilibrium expression

$$\theta_i = \frac{q_i}{q_{sat,i}} = \frac{K_i P_i}{1 + \sum_{i=1}^{nc} K_i P_i} \quad (6)$$

where the elements of the matrix $[B]$ were

$$B_{ii} = \frac{1}{D_i^S} + \sum_{j=1}^n \frac{\theta_j}{D_{ij}^S} \quad (7)$$

$$B_{ij} = -\frac{\theta_i}{D_{ij}^S} \quad (8)$$

Based on the Vignes empirical approach, for estimating the molecule interaction diffusivities D_{ij} , the following logarithmic interpolation is used,

$$D_{ij}^S = [D_i^S]^{\theta_i/(\theta_i+\theta_j)} [D_j^S]^{\theta_j/(\theta_i+\theta_j)} \quad (9)$$

and the temperature dependence of the surface diffusion coefficient is expressed as,

$$D_i^S = D_{oi} \exp\left[-\frac{E_{Ai}^S}{RT}\right] \quad (10)$$

An ODE solver in Matlab 6.5 was used to solve the differential equations of the membrane reactor model while the method of lines was used to resolve the mass transport through the membrane.

RESULTS AND DISCUSSION

Reference case for silicalite-1 membrane reactor simulation

A reference case was chosen with the catalyst mass, W of 5 kg, a membrane area per kg catalyst, A_s of 0.1 m²/kg, the

membrane thickness of 40 μm , the isothermal reactor temperature of 180°C, and the total reactor and sweep pressures of 2 and 1 atm, respectively. Based on our preliminary simulations over a range of conditions the reference case was found to be close to the best possible conditions. Starting from this case, the effects of temperature, reactor total pressure, catalyst mass and membrane thickness on the reactor behavior will be demonstrated and discussed. The reactor performance was evaluated based on the outlet CO concentration and H₂ recovery. For comparison, the corresponding operation of a conventional WGS reactor with no membrane was also considered by simulating the WGS membrane reactor with the gas permeability set to be zero. The H₂ recovery was then defined as

$$\text{H}_2 \text{ Recovery} = \frac{\text{H}_2 \text{ flow rate from membrane reactor}}{\text{H}_2 \text{ flow rate from conventional reactor}} \times 100\% \quad (11)$$

We have chosen a minimum acceptable condition as when the H₂ flow out from the membrane reactor is similar to the H₂ in the feed which corresponds to an H₂ recovery of about 78% for the reference case conditions.

The results of the simulation of the membrane reactor at the reference case conditions are presented in Table 3, Figure 3 and 4. The modeling results showed that this membrane reactor could decrease CO concentration from 9.9% to 1784 ppm with the H₂ recovery of 88.97%. The profiles of the molar flow rates of gases along the reactor can also be seen in Figure 3. For H₂ and CO₂ the flow rate profiles were compared with those for the conventional WGS reactor result. Along with a significant CO₂ removal, the membrane reactor could also enhance the flow rate of H₂ by 12.65% from the feed condition. In this case, the H₂ recovery was 88.97% which means the hydrogen loss to the permeate side is low. For the case of the conventional WGS reactor where the gas permeabilities are zero, the exit CO concentration reached 2368 ppm, and of course the H₂ recovery was 100% because of no losses due to H₂ permeation. The outlet CO concentration from the conventional reactor was near the equilibrium result, thus the lower CO concentration from the membrane reactor is achieved by circumventing the equilibrium by CO₂ removal.

Table 3. Membrane reactor performance at reference case condition

| Reference Case Condition | | Outlet CO concentration (ppm) | H ₂ Recovery (%) |
|----------------------------------|------------------------|-------------------------------|-----------------------------|
| Permeate total pressure | 1 atm | | |
| Reactor total pressure, P | 2 atm | | |
| Temperature, T | 180°C | | |
| Catalyst mass, W | 5 kg | 1784 | 88.97 |
| Membrane area/kg catalyst, A_s | 0.1 m ² /kg | 2368* | |
| Membrane thickness, L | 40 μm | | |

*) conventional WGS reactor (no membrane)

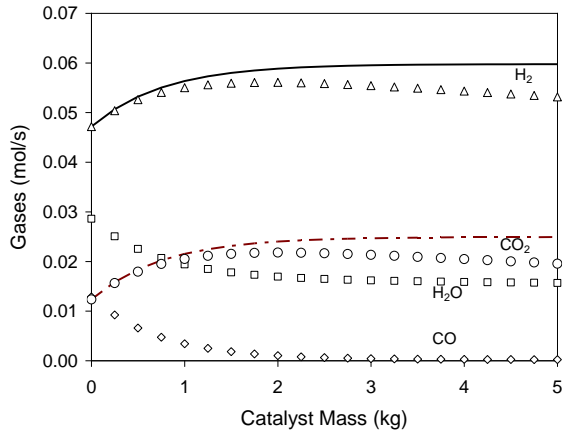


Figure 3. Gas flowrate profiles along the membrane reactor (lines are results for the conventional reactor and symbols are results for the membrane reactor)

Figure 4 shows the gas flux profiles of all components through the membrane and along the membrane reactor. The modeling results showed that H₂ had the highest flux compared to other components. H₂ flux is favoured because the concentration of H₂ in the reactor is highest which also gives it the highest driving force for transport through the membrane. The negative fluxes of N₂ and O₂ means that their permeations occur from the sweep gas to the reactor side because their concentrations in the permeate/sweep gas are higher than that in the reactor. At the permeate side the N₂ and O₂ concentration were about 80 and 20% respectively. Along the reactor the N₂ concentrations varied between 22-25% and that for O₂ varied between 0-1.6%. In terms of separation factor which is defined as the flux ratio divided by the mole fraction ratio,

$$\text{CO}_2/\text{H}_2 \text{ separation factor} = \frac{\left[\frac{J_{\text{CO}_2}}{J_{\text{H}_2}} \right]}{\left[\frac{x_{\text{CO}_2}}{x_{\text{H}_2}} \right]} \quad (12)$$

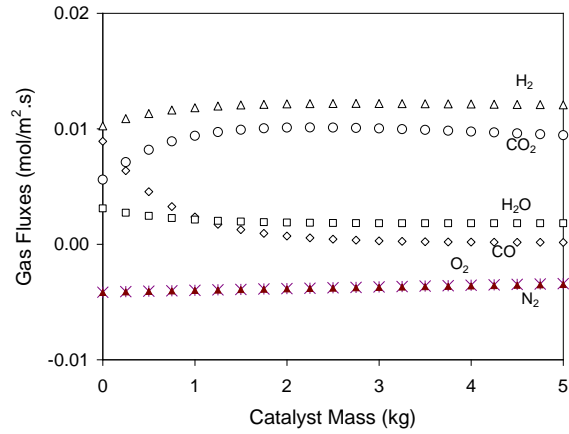


Figure 4. Gas flux profiles along the membrane reactor (the lines are results for the conventional reactor and symbols are results for the membrane reactor)

the CO₂/H₂ separation factor was found to be higher than unity as depicted later in Figure 6 with the 180°C curve.

Effect of temperature

To study the effect of temperature on the membrane reactor behavior, seven different temperatures ranging from 140 to 200°C were used in the calculations while other parameters for the reference case were kept constant. The simulations were performed to determine at which temperature the outlet CO concentration reaches a minimum and how significant the improvements are compared to the conventional reactor or the equilibrium condition. Figure 5 shows the outlet CO concentration as a function of temperature at three different reactor conditions; WGS reactor with membrane; WGS reactor without membrane (conventional WGS reactor) and WGS reaction at equilibrium condition. The H₂ recovery for the membrane reactor is also presented at different temperatures. From Figure 5 it can be seen that by increasing the temperature the outlet CO concentration

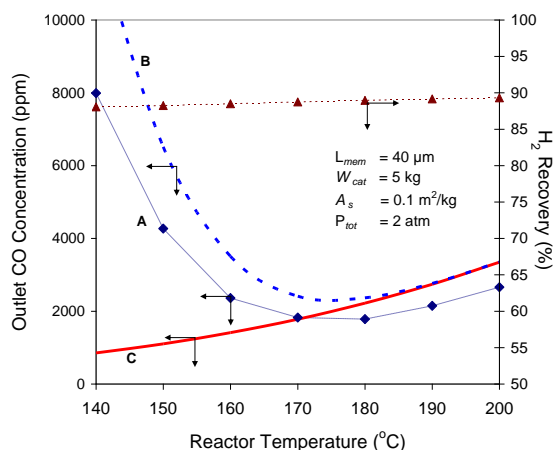


Figure 5. Outlet CO concentration for WGS reaction with (A), without (B) membrane, and equilibrium condition (C) at different temperatures (left y-ordinate); H₂ recovery for WGS membrane reactor at different temperatures (right y-ordinate)

from the membrane reactor was decreased from about 8000 ppm at 140°C, approaching the equilibrium about 1825 ppm and a minimum at 180°C (1784 ppm) and increasing again to 2660 ppm at 200°C.

As depicted also in Figure 5, the use of the membrane reactor could decrease the outlet CO concentration below that for the conventional reactor and equilibrium condition at temperatures higher than 170°C. Below 170°C, the outlet CO concentration increased for both membrane and conventional reactors because the rate of the WGS reaction decreased, however above 180°C the CO concentration increased because equilibrium was reached in the reactors. The outlet CO concentration achieved from the membrane reactor was always lower than that for the conventional reactor both when the reaction was kinetically and equilibrium limited. By increasing the temperature the H₂ recovery did not change significantly and varied between 88 to 90%. Over the temperature

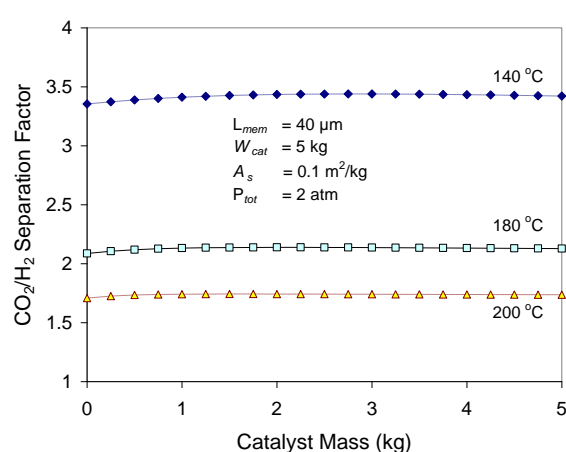


Figure 6. CO₂/H₂ separation factor along the membrane reactor at three different temperatures

range studied the H₂ recovery was always higher than the minimum target (78%).

Figure 6 shows the membrane CO₂/H₂ separation factor profiles along the reactor at three different temperatures. As stated previously, the mass transport through the membrane is modeled by surface diffusion. Based on that model it can be clearly seen that at lower temperature the membrane CO₂/H₂ selectivity is higher. This is due to the differences in strength of adsorption of these two gases. At lower temperature the stronger adsorbed molecule (CO₂) covers more of the surface, making it less accessible for H₂. However, by increasing the temperature this effect diminishes due to the temperature dependence of the adsorption coefficients. This phenomena also results in the larger differences in the CO outlet concentrations between membrane and conventional reactors at lower temperature as evident from curves A and B in Figure 5. Based on the simulation results, the CO₂/H₂ separation factors

obtained were higher than unity and thus the membrane was always slightly CO₂ selective, over the temperature range studied.

Effect of reactor total pressure

The total reactor pressure values of 1, 2, 3, 4 and 5 atm were applied in the model to study the impact of total pressure on the membrane reactor performance while the other parameters for the reference case were kept constant. The pressure on the sweep gas side was always maintained at 1 atm. As shown in Figure 7 the curves for outlet CO concentration and H₂ recovery showed consistent trends. Both the outlet CO concentration and H₂ recovery decreased as the reactor total pressure increased. Changing total pressure will not affect the equilibrium conversion of CO because the total mole coefficient of the reactants and products in the WGS reaction are equal. The decrease in outlet CO concentration is mainly due to changes in the gas permeation which are dependent on the total pressure. The mass transport which is based on the surface diffusion mechanism will increase if the total pressure increases

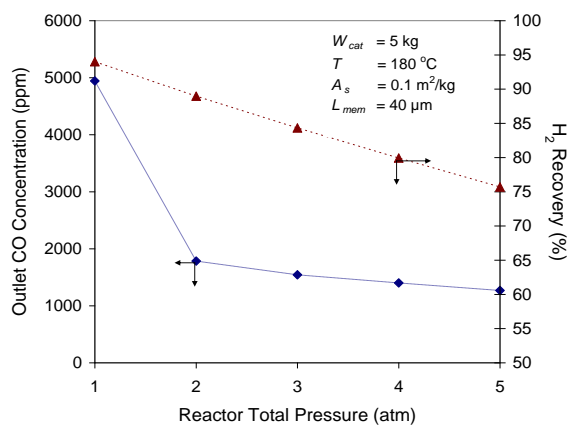


Figure 7. Outlet CO concentration and H₂ recovery as function of reactor total pressures

because the driving force for diffusion is increased. The H₂ recovery was found to vary between 75 to 95% which still within a tolerable range. As depicted in Figure 7, the outlet CO concentration decreased drastically from the reactor total pressure of 1 to 2 atm, and continued to decreased, but at a lower rate from 2 to 5 atm. Considering costs for gas compression and the fact that the outlet CO concentration decreases less beyond 2 atm, but with the same reduction in the H₂ recovery, setting the reactor total pressure at 2 atm is a reasonable choice.

Effect of catalyst mass

The catalyst mass was varied from 1 to 6 kg while all other parameters were kept constant at the reference case settings. Figure 8 illustrates the effect of catalyst mass on the outlet CO concentration and H₂ recovery. The outlet CO concentration decreased as the catalyst mass increased. H₂ recovery moderately decreased with increasing catalyst mass and was at all conditions higher than the minimum target. The higher outlet CO concentration at lower catalyst mass was due to the lower CO conversion and the correspondingly smaller

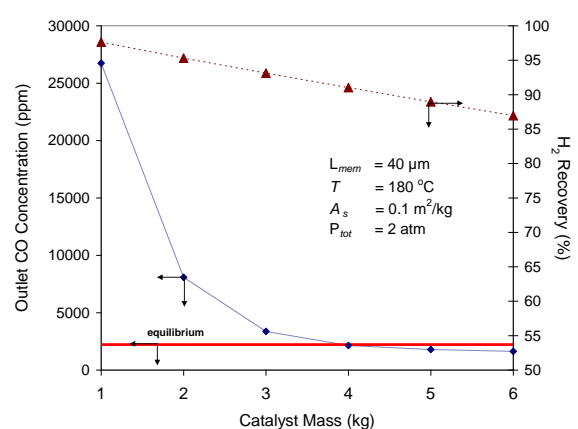


Figure 8. Outlet CO concentration and H₂ recovery as function of catalyst mass

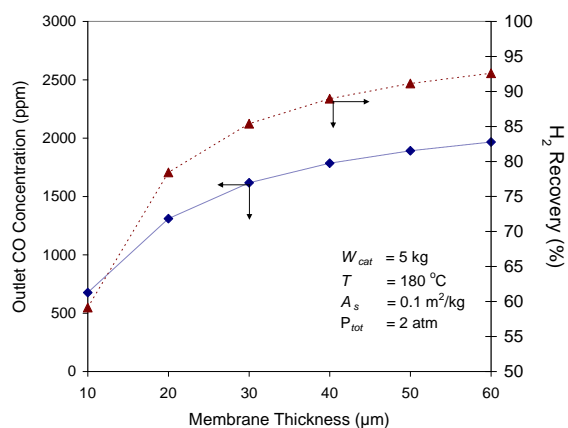


Figure 9. Outlet CO concentration and H₂ recovery as function of membrane thickness

membrane area (membrane area to catalyst mass was constant at 0.1 m²/kg) which resulted in less CO₂ removal and was not sufficient to break the equilibrium of the WGS reaction. The larger membrane area at higher catalyst mass also resulted in a reduction in the H₂ recovery. As depicted in Figure 8, the outlet CO concentration decreased drastically from the catalyst mass of 1 to 3 kg and continued to decrease, although by a smaller amount, from 4 to 6 kg. Considering the reduction in the outlet CO concentration is less beyond 4 kg but with the same reduction in the H₂ recovery the catalyst mass of 5 kg appears to be reasonable choice because at that point the outlet CO concentration was found lower than that achieved by the equilibrium WGS conventional reactor.

Effect of membrane thickness

The membrane thickness was varied from 10 to 60 μm to study its effect on the membrane reactor performance. The other parameters for the reference case were kept constant. Figure 9 illustrates the effect of membrane thickness on the outlet CO

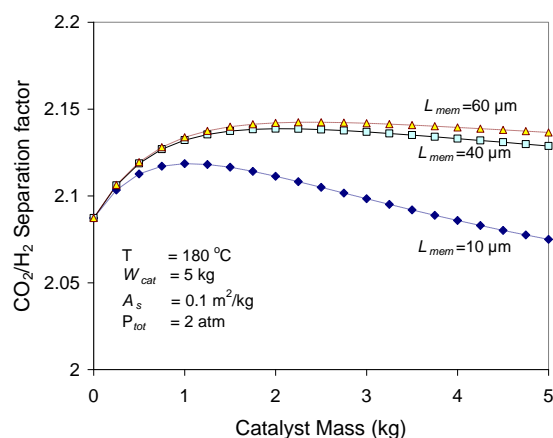


Figure 10. CO₂/H₂ separation factor along the membrane reactor at three different membrane thicknesses

concentration and H₂ recovery. The outlet CO concentration and H₂ recovery increased as the membrane thickness increased. As the membrane thickness increased the gas permeation fluxes were decreased. The CO₂ removal became less significant to force the chemical equilibrium of the WGS reaction to the product side, resulting in a lower CO consumption and higher outlet CO concentration. On the other hand, H₂ recovery increased with membrane thickness because the lower flux resulted in less H₂ permeating to the sweep gas. From Figure 9 it can be seen that at a membrane thickness of 20 μm the outlet CO concentration reached 1310 ppm with 78.44% of H₂ recovery. However, at a membrane thickness of 10 μm the outlet CO concentration was down to 675 ppm, but the H₂ recovery was only about 59% which is much lower than the minimum target 78%. At this condition, about 25% of the H₂ entering the reactor is lost.

Figure 10 shows the membrane CO₂/H₂ separation factor profiles along the reactor at three different membrane thicknesses. As the membrane thickness was varied the

CO₂/H₂ separation factor did not change substantially, particularly for a membrane thickness greater than 40 μm. However, when the membrane thickness increased from 10 to 60 μm the CO₂/H₂ separation factor slightly improved from 2.07 to 2.15. It is also evident from the results in Figure 9 that the increase in the CO₂/H₂ separation factor is largest for increasing the membrane thickness from 10 to 40 μm, because it is over this range of membrane thickness where the H₂ recovery increases the most with a relatively lesser increase in the outlet CO concentration. Beyond a membrane thickness of 40 μm, the H₂ recovery and outlet CO concentration appear to increase at about equal rates with membrane thickness.

Best performance of wgs membrane reactor

Based on the overall modeling and simulation of the WGS membrane reactor, by varying the operating parameters, the best performance of the membrane reactor is presented in Table 4. It is apparent from this modeling study that although the WGS equilibrium can be circumvented, sufficiently low outlet CO concentrations are not

obtained with the membrane reactor to produce a product gas for direct feed to a PEM fuel cell. Lower outlet CO concentrations than about 1300 ppm are only achievable with an unacceptably low H₂ recovery. These deficiencies stem from the poor selective transport of CO₂ versus H₂ that is achievable with the silicalite-1 membrane. There are materials related to silicalite-1 that have higher adsorption affinities for CO₂, and thus potentially could provide higher CO₂ permeation selectivity. We have found that the cations in NaZSM-5 and Ba-ZSM-5 act as additional sites for stronger adsorption of CO₂ (Wirawan and Creaser, 2006b). Also, chemical modification of MFI zeolite with amine compounds forms additional sites with a strong basic character that enhances adsorption of CO₂ (Guo *et al*, 2006). From our simulations we have found that an increase in the enthalpy of adsorption of CO₂ by 50% (all other parameters unchanged) allowed the outlet CO concentration to reach below 300 ppm with an acceptable H₂ recovery at the reference case conditions. However, although MFI materials exist with the potential for improved selective adsorption and transport

Table 4. Best silicalite-1 membrane reactor performance

| Operation Condition | | Outlet CO concentration (ppm) | H ₂ Recovery (%) |
|---|------------------------|-------------------------------|-----------------------------|
| Permeate total pressure | 1 atm | | |
| Reactor total pressure, <i>P</i> | 2 atm | | |
| Temperature, <i>T</i> | 180 °C | | |
| Catalyst mass, <i>W</i> | 5 kg | 1310 | 78.44 |
| Membrane area/kg catalyst, <i>A_s</i> | 0.1 m ² /kg | 100* | 78* |
| Membrane thickness, <i>L</i> | 20 μm | | |

*) target for PEM fuel cell

of CO₂, it is not known at this time how these additional sites for enhanced CO₂ adsorption will influence the adsorption and diffusion of other species. For example, silicalite-1 membranes simply impregnated with CaO, were found to have enhanced adsorption of CO₂ via the formation of carbonates and they appeared to have better selective transport of CO₂ from CO₂/H₂ mixtures (Lindmark *et al*, 2010). However, the permeance of all species through these membranes was greatly reduced due to the blockage of pores by the carbonate compounds.

CONCLUSIONS

Based on a modeling study of a WGS membrane reactor with a silicalite-1 membrane, a CO concentration of about 1310 ppm and a H₂ recovery of 78.44% are achievable from a typical autothermal steam reforming product composition. As the temperature increased the CO₂/H₂ selectivity decreased but in combination with the WGS reaction kinetics this resulted in a minimum outlet CO concentration within the temperature range studied. Increasing the total pressure in the reactor increased the driving force for the permeation, but did not improve the CO₂ removal significantly. Increasing the membrane thickness increased the outlet CO concentration and H₂ recovery and slightly enhanced the CO₂/H₂ selectivity but decreased the permeation fluxes which corresponded to a larger required membrane area. Generally, the modeling study showed that both the WGS reaction rate and the CO₂/H₂ permeation played an important role for the overall reactor performance. The membrane

reactor could achieve lower outlet CO concentration than the equivalent equilibrium composition, however the CO concentration could not be lowered in a single step to levels required for a PEM fuel cell with an acceptable H₂ recovery. This is due to the fact that sufficiently high CO₂/H₂ selective permeation cannot be achieved with a silicalite-1 membrane.

NOMENCLATURE

Roman symbols

A_s : membrane area, m²/kg catalyst

[B] : square matrix of inverse Maxwell-Stefan coefficients, m⁻²·s

D : diffusivity, m²·s⁻¹

E_A : activation energy, J·mol⁻¹

J : permeation flux, mol·m⁻²·s⁻¹

L : membrane thickness, m

n : molar flowrate mol·s⁻¹

nc : number of component

P : total pressure, bar

q : molar loading, mol·kg⁻¹

q_{sat} : saturation loading, mol·kg⁻¹

q_{tot} : total loading, mol·kg⁻¹

R : universal gas constant, bar·m³·mol⁻¹·K⁻¹.

T : temperature, °C.

Greek symbols

ρ : density, kg·m⁻³.

θ : fractional occupancy, (-)

[Γ]: matrix of thermodynamic factor, (-)

Subscript

T : function of temperature

i : component i

j : component j

Superscript

S : surface diffusion

ACKNOWLEDGEMENT

The authors are grateful for the financial support of the Swedish Energy Agency and the SIDA-Swedish Research Links program.

REFERENCES

1. Algieri, C., Bernardo, P., Golemme, G., Barbieri, G. and Drioli, E. (2003) Permeation properties of a thin silicalite-1 (MFI) membrane. *J. Membr. Sci.*, 222, 181.
 2. Bakker, W. J., Broeke, L. J. P. V. D., Kapteijn, F. and Moulijn, J. (1997) Temperature dependence of one-component permeation through a silicalite-1 membrane. *AIChE J.*, 43, 2203.
 3. Basile, A., Paturzo, L. and Gallucci, F. (2003) Co-current and counter-current modes for water gas shift membrane reactor. *Catal. Today*, 82, 275–281.
 4. Brunetti, A., Caravella, A., Barbieri, G. and Drioli, E. (2007) Simulation study of water gas shift reaction in a membrane reactor. *J. Membrane Sci.*, 306, 329.
 5. Bussai, C., Vasenkov, S., Liu, H., Böhlmann, W., Fritzsche, S., Hannongbua, S., Haberlandt, R. and Kärger, J. (2002) On the diffusion of water in silicalite-1: MD simulations using ab initio fitted potential and PFG NMR measurements. *Appl. Catal. A: Gen.*, 232, 59.
 6. Ciavarella, P., Moueddeb, H., Miachon, S., Fiaty, K. and Dalmon, J.-A. (2000) Experimental study and numerical simulation of hydrogen/isobutane permeation and separation using MFI-zeolite membrane reactor. *Catal. Today*, 56, 253.
 7. Dunne, J. A., Mariwala, R., Rao, M., Sircar, S., Gorte, R. J. and Myers, A. L. (1996) Calorimetric Heats of Adsorption and Adsorption Isotherms. 1. O₂, N₂, Ar, CO₂, CH₄, C₂H₆, and SF₆ on Silicalite. *Langmuir*, 12, 5888.
 8. Fleys, M. and Thompson, R. W. (2005) Monte Carlo Simulations of Water Adsorption Isotherms in Silicalite and Dealuminated Zeolite Y. *J. Chem. Theory Comput.*, 1, 453.
 9. Graaf, J. M. V. D., Kapteijn, F. and Moulijn, J. A. (1999) Modeling permeation of binary mixtures through zeolite membranes. *AIChE J.*, 45, 497.
 10. Guo, J., Han, A. J., Yu, H., Dong, J. P., He, H. and Long, Y. C. (2006) Base property of high silica MFI zeolites modified with various alkyl amines. *Micropor. Mesopor Mater.*, 94, 166.
 11. Hedlund, J., Sterte, J., Anthonis, M., Bons, A., Cartensen, B., Corcoran, N., Cox, D., Deckman, H., Gijst, W. D., Moor, P., Lai, F., Machenry, J., Mortier, W., Reinoso, J. and Peters, J. (2002) High-flux MFI membranes. *Micropor. Mesopor Mater.*, 52, 179.
 12. Huang, J., El-Azzami, L. and Ho, W. S. W. (2005) Modeling of CO₂-selective water gas shift membrane reactor for fuel cell. *J. Membrane Sci.*, 261, 67.
 13. Kapteijn, F., Bakker, W. J. W., Graaf, J. V. D., Zheng, G., Poppe, J. and Moulijn, J. A. (1995) Permeation and separation behavior of a silicalite-1 membrane. *Catal. Today*, 25, 213.
 14. Kärger, J., Pfeifer, H. and Stallmach, F. (1993) ¹²⁹Xe and ¹³C PFG n.m.r. study of the intracrystalline self-diffusion of Xe, CO₂, and CO. *Zeolites*, 13, 50.
 15. Keiski, R. L., Desponds, O., Chang, Y. F. and Somorjai, G. A. (1993) Kinetics of the
-

-
- water-gas shift reaction over several alkane activation and water-gas shift catalysts. *Appl. Catal. A: Gen.*, 101, 317.
16. Krishna, R. and Baur, R. (2003) Modelling issues in zeolite based separation processes. *Sep. Pur. Technol.*, 33, 213.
17. Krishna, R. and Wesselingh, J. A. (1997) The Maxwell-Stefan approach to mass transfer. *Chem. Eng. Sci.*, 52, 861.
18. Lindmark, J., Hedlund, J., K. Wirawan, S. and Creaser, D. (2010) Impregnated Silicalite-1 Membranes for Enhanced selectivity. *J. Membr. Sci.*, 365 (1-2), 188-197
19. Miachon, S., Ciavarella, P., Dyk, L. V., Kumakiri, I., Fiaty, K., Schuurman, Y. and Dalmon, J.-A. (2007) Nanocomposite MFI-alumina membranes via pore-plugging synthesis: Specific transport and separation properties. *J. Membr. Sci.*, 298, 71.
20. Nagumo, R., Takaba, H., Suzuki, S. and Nakao, S. (2001) Estimation of inorganic gas permeability through an MFI-type silicalite membrane by a molecular simulation technique combined with permeation theory. *Micropor. Mesopor Mater*, 48, 247.
21. Papadopoulos, G. K., Jobic, H. and Theodorou, D. N. (2004) Transport Diffusivity of N₂ and CO₂ in Silicalite: Coherent Quasielastic Neutron Scattering Measurements and Molecular Dynamics Simulations. *J. Phys. Chem. B*, 108, 12748.
22. Salmi, T. and Hakkarainen, R. (1989) Kinetic Study of the Low-Temperature Water-Gas Shift Reaction over a Cu-ZnO Catalyst. *Appl. Catal.*, 49 285.
23. Skoulidas, A. I. and Sholl, D. S. (2002) Transport Diffusivities of CH₄, CF₄, He, Ne, Ar, Xe, and SF₆ in Silicalite from Atomistic Simulations. *J. Phys. Chem. B*, 106, 5061.
24. Wirawan, S. K. and Creaser, D. (2006a) CO₂ adsorption on silicalite-1 and cation exchanged ZSM-5 zeolites using a step change response method. *Micropor. Mesopor Mater*, 91, 196.
25. Wirawan, S. K. and Creaser, D. (2006b) Multicomponent H₂/CO/CO₂ adsorption on BaZSM-5 zeolite. *Sep. Pur. Technol.*, 52, 224.
26. Wirawan, S. K., Creaser, D., Lindmark, J., Hedlund, J., Bendiyasa, I. M. and Sediawan, W. B. (2011) H₂/CO₂ Permeation through a Silicalite-1 Composite Membrane, *J. Membr. Sci.* 375 (1-2), 313-322
27. Zalc, J. M. and Löffler, D. G. (2002) Fuel processing for PEM fuel cells: transport and kinetic issues of system design. *J. Power Sources*, 111, 58.
-